



# Interplay between intensity-dependent dispersion and Kerr nonlinearity on the soliton formation

JEN-HSU CHANG,<sup>1</sup> CHUN-YAN LIN,<sup>2</sup> AND RAY-KUANG LEE<sup>2,3,4,5,\*</sup>

<sup>1</sup>Graduate School of National Defense, National Defense University, Taoyuan City 335, Taiwan

<sup>2</sup>Institute of Photonics Technologies, National Tsing Hua University, Hsinchu 30013, Taiwan

<sup>3</sup>Department of Physics, National Tsing Hua University, Hsinchu 30013, Taiwan

<sup>4</sup>Physics Division, National Center for Theoretical Sciences, Taipei 10617, Taiwan

<sup>5</sup>Center for Quantum Technology, Hsinchu 30013, Taiwan

\*rkleee@ee.nthu.edu.tw

Received 24 May 2023; revised 19 July 2023; accepted 20 July 2023; posted 21 July 2023; published 4 August 2023

**A generalized nonlinear Schrödinger equation is studied with the interplay between Kerr nonlinearity and intensity-dependent dispersion. The supported soliton solutions are characterized analytically in different families by the pseudo-potential method, in terms of Maimistov and Cuspon solitons for different ratio between the intensity-dependent dispersion and Kerr nonlinearity. Direct numerical simulations also agree with our analytical formulas. In addition to the well-studied Kerr-type nonlinearity, our results reveal an unexplored scenario with the introduction of the nonlinear corrections to wave dispersion.** © 2023 Optica Publishing Group

<https://doi.org/10.1364/OL.496186>

**Introduction.** The nonlinear Schrödinger equation (NLSE) with Kerr (or cubic) nonlinearity is the main governing equation for the evolution of optical fields in a nonlinear medium [1]. For pulse propagation in optical fibers, temporal solitons are supported with the balance between the group velocity dispersion and self-phase modulation [2]. To utilize solitons for light wave systems, dispersion managements, including dispersion-decreasing fibers and periodic dispersion maps, are commonly employed for modern wavelength division multiplexing [3].

In addition to the linear dispersion, nonlinear corrections to the chromatic dispersion as a function of the wave intensity have been reported for water and acoustic waves [4–6]. For optical systems, the photon–atom interactions in general bring the nonlinear dispersion effects [7–11]. With intensity-dependent dispersion only, the supported soliton solutions are formed due to the interplay between the constant coefficient dispersion and the intensity-dependent dispersion, leading to a continuous family of solitary wave solutions [12,13].

In this paper, we show that soliton solutions exist due to the interplay between intensity-dependent dispersion and Kerr nonlinearity on the soliton formation. Here, we consider a generalized NLSE with both Kerr nonlinearity characterized by the coefficient  $g$ , and the nonlinear dispersion characterized by  $b$ , as follows:

$$i\psi_z + \psi_{xx} = b|\psi|^2\psi_{xx} + g|\psi|^2\psi. \quad (1)$$

When  $b = 0$  and  $g < 0$  (or  $g > 0$ ), Eq. (1) corresponds to the focusing (defocusing) NLSE, which supports bright (dark) solitons. Moreover, in the case  $g = -2(1 - b)$ , Eq. (1) gives the continuous limit of the Salerno model [14]. When one considers a strong coupling between nonlinearity and diffraction in a crystal at the super-collimation point, our model equation can also be mapped to a nonlinear diffraction in NLSE [15,16].

**Model equation.** The corresponding Lagrangian density for Eq. (1) has the form

$$L = \left( \frac{i(\psi_z\bar{\psi} - \bar{\psi}_z\psi)}{2b|\psi|^2} - \frac{g}{b^2} \right) \ln | -1 + b|\psi|^2 | - \frac{g}{b} |\psi|^2 + |\psi_x|^2, \quad (2)$$

which also keeps the  $U(1)$  symmetry, i.e.,  $\psi \rightarrow e^{i\theta}\psi$ . With the help of Noether's theorem [17], there are two conserved quantities for our model equation, denoted as the density  $Q$  and the Hamiltonian  $H$ :

$$Q = \frac{1}{b} \int_{-\infty}^{\infty} \ln | -1 + b|\psi|^2 | dx; \quad (3)$$

and

$$H = \int_{-\infty}^{\infty} \left( -\frac{g}{b^2} (\ln | -1 + b|\psi|^2 |) - \frac{g}{b} |\psi|^2 + |\psi_x|^2 \right) dx. \quad (4)$$

When the nonlinear dispersion term vanishes, i.e.,  $b \rightarrow 0$ , the conserved density  $Q$  in Eq. (3) approaches  $\int_{-\infty}^{\infty} |\psi|^2 dx$ ; while  $H$  in Eq. (4) becomes the Hamiltonian  $\int_{-\infty}^{\infty} (|\psi_x|^2 + \frac{g}{2} |\psi|^4) dx$  of NLSE. In contrast to NLSE, it is noteworthy that Eq. (1) is not a Hamiltonian system by a direct calculation.

To find the stationary soliton solution, we assume  $\psi = p(x)e^{-icz}$  with the wavenumber  $c$  and the real function  $p(x)$  to be determined. Plugging this form into Eq. (1), one has

$$p''(x) = \frac{cp(x) - gp(x)^3}{-1 + bp(x)^2}. \quad (5)$$

By rewriting Eq. (5) as

$$p''(x) = -\frac{dV(p)}{dp} \quad \text{or} \quad \frac{1}{2} \left( \frac{dp}{dx} \right)^2 = -V(p), \quad (6)$$

the pseudo-potential  $V(p)$  can be derived,

$$V(p) = - \int \frac{cp - gp^3}{bp^2 - 1} dp = \frac{gp^2}{2b} - \frac{c - \frac{g}{b}}{2b} \ln |bp^2 - 1|, \quad (7)$$

with  $V(0) = 0$ . When  $b > 0$ , we see that there is a vertical asymptote at  $p = \frac{1}{\sqrt{b}}$ , which differs from a generally smooth pseudo-potential. Even though  $\omega \equiv \frac{bc}{g} = 1$  makes the conserved density  $Q$  divergent, we assume  $\frac{bc}{g} \neq 1$ , along with  $g < 0, b > 0$ , and  $c < 0$ , to test the convergence of Eq. (3). For a bounded solution, we ask for  $0 < p(0) = M$  and have

$$Q = \frac{-1}{b} \int_0^1 \frac{\ln u du}{\sqrt{\frac{-2g}{b}(1-u) |1-u + (1-\omega) \ln u|}} - \frac{1}{b} \int_0^1 \frac{\ln u_1 du_1}{\sqrt{\frac{-2g}{b}(1+u_1) |1+u_1 + (1-\omega) \ln u_1|}} + \frac{1}{b} \int_1^{bM^2-1} \frac{\ln u_1 du_1}{\sqrt{\frac{-2g}{b}(1+u_1) |1+u_1 + (1-\omega) \ln u_1|}}, \quad (8)$$

where  $u = 1 - bp^2$  and  $u_1 = bp^2 - 1$ . The convergence near  $u = 0$  and  $u = 1$  can be obtained similarly as that done in Ref. [12]. When the denominator is zero, we can consider the integral  $\int_0^{\mu_1} \kappa \frac{d\mu}{\sqrt{|\mu|}}, \kappa > 0, \mu_1 > 0$ , and it is convergent.

**Maimistov Solitons.** According to the pseudo-potential theory, if the first positive root, denoted as  $\Omega$ , of  $V(p)$  exists, then  $\sqrt{\Omega}$  is the corresponding amplitude of the soliton [18,19]. Next, we investigate the first root  $\Omega$ . As the translation invariant of Eq. (5) is valid, we also assume the amplitude happens at  $x = 0$ . Now, one has the equation

$$p^2(x) = \left(\frac{c}{g} - \frac{1}{b}\right) \ln |bx - 1|. \quad (9)$$

In this case, we have two positive roots in general. Here, we focus on the first positive root, i.e.,

$$\Omega = \frac{1}{b} \left[ -\frac{1}{\gamma} W(\gamma e^\gamma) + 1 \right] \leq \frac{1}{b}, \quad (10)$$

where  $\gamma \equiv 1/(\omega - 1)$  and  $W(x)$  is the Lambert function. If we consider the approximation

$$p''(x) \approx -cp(x) + g \left(1 - \frac{bc}{g}\right) p(x)^3 + bg \left(1 - \frac{bc}{g}\right) p(x)^5. \quad (11)$$

Equation (11) is the type of quintic Duffing equation, which supports the Maimistov soliton solution [20]. The corresponding soliton solution has the form

$$p^2(x) = \frac{-2c}{\frac{bc-g}{2} + \sqrt{\frac{(g-bc)^2}{4} - \frac{4}{3}bc(bc-g) \cosh(2\sqrt{-cx})}}. \quad (12)$$

When  $b = 0, g = -1, c = \frac{-1}{2}$ , we have the NLSE one soliton solution, i.e.,  $p(x) = 1/[1/2 + 1/2 \cosh(x/\sqrt{2})]$ . Moreover, to have a bounded solution, we ask for  $bp^2(x) \leq bp^2(0) \leq 1$  with the following equation:

$$bp^2(0) = 12 \frac{\omega}{-3\omega + \sqrt{-39\omega^2 + 30\omega + 9} + 3}, \quad (13)$$

which results in  $0 \leq \omega \leq \frac{5}{11} \equiv \omega_1$ .

**Cuspon solutions.** From Eq. (6), one notes that  $p(0) = \frac{1}{\sqrt{b}}$  and  $p(\pm\infty) = 0$ , then we have

$$|x| = \int_p^{\frac{1}{\sqrt{b}}} \frac{d\xi}{\sqrt{|\frac{-g\xi^2}{b} + \frac{bc-g}{b^2} \ln(1-b\xi^2)|}}. \quad (14)$$

To obtain an approximation of a Cuspon solution, one can consider the asymptotic limit with the Taylor expansion near  $x = 0$  and arrive at [12]

$$|x| = \int_p^{p(0)=\frac{1}{\sqrt{b}}} \frac{dp}{\sqrt{-cp(1 + \frac{b-g/c}{2}p^2 + \dots)^{1/2}}} = \frac{-1}{\sqrt{-c}} \ln p - \frac{b-g/c}{8\sqrt{-c}} p^2 - \dots. \quad (15)$$

Consequently, one yields the approximation of a Cuspon solution

$$p(x) \approx e^{-\frac{1}{2}W(\frac{bc-g}{4c}e^{-2|x|\sqrt{-c}})-|x|\sqrt{-c}}, \quad (16)$$

where  $W$  again is the Lambert function. Since  $\frac{bc-g}{4c}$  is nonnegative, the approximation Eq. (16) is applicable for all  $x$ . The corresponding amplitude is  $p(0) = e^{-\frac{1}{2}W(\frac{bc-g}{4c})}$ . By Eq. (16), if  $\frac{bc}{g} = 1$ , one has the Peakon solution

$$p(x) = e^{-\sqrt{\frac{-g}{b}}|x|}. \quad (17)$$

Regarding the applicable range to keep the validity of Eq. (16), let us have

$$p(0) = e^{-\frac{1}{2}W[\frac{bc-g}{4c}]} = \frac{1}{\sqrt{b}} = e^{-\frac{\ln b}{2}},$$

resulting in

$$W\left[\frac{bc-g}{4c}\right] = \ln b \quad \text{or} \quad e^{W(\frac{1}{4}(b-\frac{g}{c}))} = b. \quad (18)$$

By the property of the Lambert function  $e^{W(y)} = \frac{y}{W(y)}$ , the solution of Eq. (18) is

$$\frac{1}{4} \left(b - \frac{g}{c}\right) = 0 \quad \text{or} \quad b \ln b.$$

When  $\frac{bc-g}{4c} = 0$ , one has Eq. (17). If  $\frac{bc-g}{4c} = b \ln b$ , then one yields

$$0 < \frac{g}{c} = b(1 - 4 \ln b). \quad (19)$$

Also,  $1 < w = \frac{bc}{g} = \frac{1}{1-4 \ln b} \rightarrow \infty$  as  $b \rightarrow e^{1/4}$ . Thus, if we choose  $1 \leq b < e^{1/4} \approx 1.28$ , then Eq. (19) is the condition for the approximated solution given in Eq. (16) to be valid.

In Fig. 1, we illustrate the existence of soliton solutions with the interplay between intensity-dependent dispersion and Kerr nonlinearity. With the single parameter  $\omega \equiv \frac{bc}{g}$ , we plot the density  $Q$  of supported soliton solutions obtained by direct numerical simulations from Eq. (1). The numerical solutions are generated through the iteration with the Fourier spectral method, with an initial guess from the theoretical prediction. In general, the lack of a good initial guess limits the possibility to generate a converged solution. We also consider  $0 \leq \omega$  for bright solitons only. Numerically, three regions are identified (in different colors): stable Maimistov soliton solutions for  $0 \leq \omega \leq \omega_a$ ; unstable Maimistov soliton solutions and Cuspon solutions for  $\omega > 1$ . Moreover, stable Cuspon solution of amplitude  $\frac{1}{\sqrt{b}}$  and unstable smooth soliton of amplitude larger than  $\frac{1}{\sqrt{b}}$

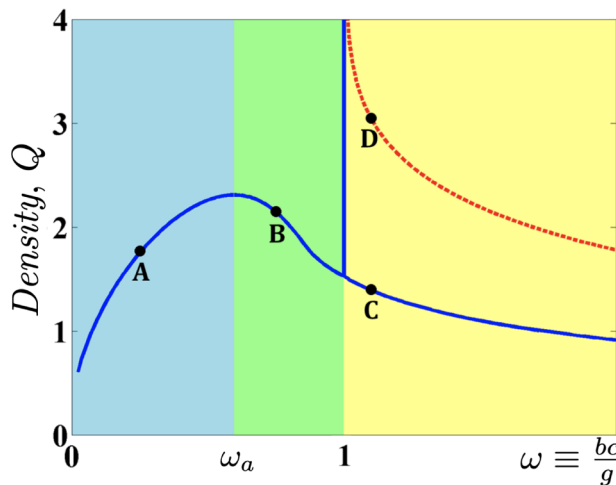


**Fig. 1.** Density  $Q$  of supported soliton solutions obtained by direct numerical simulations of Eq. (1), as a function of the parameter  $\omega \equiv \frac{bc}{g}$ . Bright solitons exist for  $0 \leq \omega$ . The numerical simulations show that if  $0 \leq \omega \leq \omega_a$ , the founded soliton solution is stable; while it is unstable for  $\omega_a < \omega < 1$ . Here, we have  $\omega_a \approx 0.6$ . Four selected examples are marked for the comparison to the analytical results shown in Fig. 2. Note that there exists a singularity located at  $\omega = 1$ .

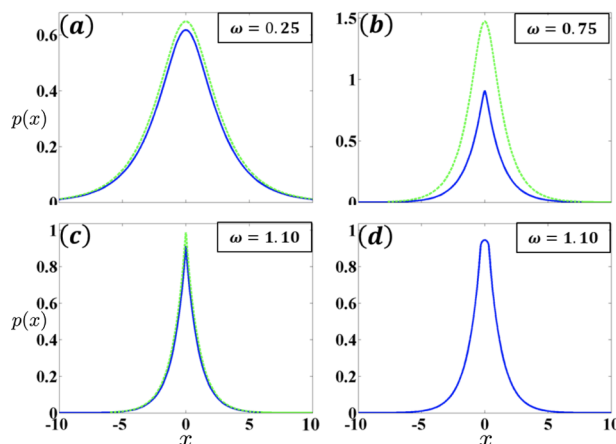


**Fig. 2.** Four selected examples for the supported solitons  $p(x)$  are illustrated: (a) stable Maimistov soliton solution for  $\omega = 0.25$ ; (b) unstable soliton solution for  $\omega = 0.75$ ; (c) stable lowest-branch Cuspon solutions for  $\omega = 1.10$ ; and (d) unstable higher-order Cuspon solution for  $\omega = 1.10$ , corresponding to the four markers A, B, C, and D in Fig. 1, respectively. Here, curves in blue color are the numerical solutions; while curves in green color are generated from the analytical formulas given in Eqs. (12) and (16) for Maimistov soliton and Cuspon solutions, respectively. Note that there is no analytical solution for the unstable smooth soliton given in (d).

exist for  $\omega > 1$  at the same time. As our analyses show, the singularity happens at  $\omega = 1$ . Moreover, compared to the analytical value of  $\omega_1 = 5/11 \approx 0.4545$ , numerically we have  $\omega_a \approx 0.6$  to support stable Maimistov soliton solutions.

Even though we have a discrepancy on the values of  $\omega_1$  and  $\omega_a$ , i.e., between the analytical and numerical results, the soliton profiles obtained from numerical results match the analytical formulas given in Eqs. (12) and (16) very well. In Fig. 2, we select four examples for the supported soliton solutions: stable

Maimistov soliton solution for  $\omega = 0.25$  [Fig. 2(a)]; unstable soliton solution for  $\omega = 0.75$  [Fig. 2(b)]; stable lowest-branch Cuspon solutions for  $\omega = 1.10$  [Fig. 2(c)]; and unstable higher-order Cuspon solution for  $\omega = 1.10$  [Fig. 2(d)], corresponding to the four markers A, B, C, and D in Fig. 1, respectively.

As one can see the curves obtained from the numerical solutions (in blue color) give good agreement with the curves generated from the analytical formulas given in Eqs. (12) and (16) (in green color), for Maimistov soliton [Fig. 2(a)] and Cuspon solutions [Fig. 2(c)], respectively. It is noted that in Fig. 2(b) a discrepancy comes from the validation of our Maimistov solution, which works only for  $\omega \leq \omega_1$ . Also, unstable smooth soliton solution [Fig. 2(d)] for  $\omega > 1$  is different from the Maimistov solution due to the amplitude. When  $g = 0$ , this unstable smooth soliton solution was already investigated in Ref. [21].

In addition to the the conserved density  $Q$  given in Eq. (3), one may apply Vakhitov–Kokolov (VK) criteria for spectral stability, i.e.,  $\frac{\partial Q(\omega)}{\partial \omega} < 0$  [22–26]. In short, for the range  $0 \leq \omega < \omega_a$ , all the supported Maimistov solitons are stable; but become unstable  $\omega_a < \omega \leq 1$ . However, the Cuspon solutions are tested numerically as stable ones, as those supported with  $g = 0$  but  $b \neq 0$  [13].

**Conclusion.** With the nonlinear correction to the dispersion, we investigate the interplay between nonlinear dispersion and Kerr nonlinearity. Approximated stationary soliton solutions, i.e., both the smooth Maimistov soliton and singular Cuspon solutions, are derived analytically by utilizing the pseudo-potential method. With the parameter  $\omega = \frac{bc}{g}$ , we identify four different regions to support numerically stable/unstable smooth solitons, and stable Cuspon solutions. The corresponding profiles of these solutions, as well as the stabilities, are also verified with direct numerical simulations. As the nonlinear corrections to wave dispersion may arise in many settings, our results pave a theoretical platform to study the rich family and the related dynamics with nonlinear dispersion.

**Funding.** National Science and Technology Council (112-2115-M-606-001, 112-2123-M-007-001).

**Acknowledgments.** This work is supported in part by the National Science and Technology Council (NSTC) of Taiwan under grant nos. NSTC 112-2115-M-606-001 and 112-2123-M-007-001.

**Disclosures.** The authors declare no conflicts of interest.

**Data availability.** No data were generated or analyzed in the presented research.

## REFERENCES

1. Yu. S. Kivshar and G. P. Agrawal, *Optical Solitons* (Academic Press, 2003).
2. G. P. Agrawal, *Nonlinear Fiber Optics*, 4th edition (Academic Press, 2007).
3. G. P. Agrawal, *Applications of Nonlinear Fiber Optics*, 2nd edition (Academic Press, 2008).
4. G. B. Whitham, *J. Fluid Mech.* **22**, 273 (1965).
5. G. B. Whitham, *Linear and Nonlinear Waves* (John Wiley & Sons, 1999).
6. V. E. Gusev, W. Lauriks, and J. Thoen, *J. Acoust. Soc. Am.* **103**, 3216 (1998).
7. A. A. Koser, P. K. Sen, and P. Sen, *J. Mod. Opt.* **56**, 1812 (2009).
8. A. Javan and A. Kelley, *IEEE J. Quant. Electron.* **2**, 470 (1966).
9. A. D. Greentree, D. Richards, J. A. Vaccaro, A. V. Durrant, S. R. de Echaniz, D. M. Segal, and J. P. Marangos, *Phys. Rev. A* **67**, 023818 (2003).

10. E. Shahmoon, P. Grisins, H. P. Stimming, I. Mazets, and G. Kurizki, *Optica* **3**, 725 (2016).
11. R. Hogan, A. Safari, G. Marcucci, B. Braverman, and R. W. Boyd, *Optica* **10**, 544 (2023).
12. C.-Y. Lin, J.-H. Chang, G. Kurizki, and R.-K. Lee, *Opt. Lett.* **45**, 1471 (2020).
13. R. M. Ross, P. G. Kevrekidis, and D. E. Pelinovsky, *Q. Appl. Math.* **79**, 641 (2021).
14. J. Gomez-Garde, B. A. Malomed, L. M. Floria, and A. R. Bishop, *Phys. Rev. E* **73**, 036608 (2006).
15. X. Jianga, C. Zhou, X. Yu, S. Fan, M. Soljacic, and J. D. Joannopoulos, *Appl. Phys. Lett.* **91**, 031105 (2007).
16. Z. Xu, B. Maes, X. Jiang, J. D. Joannopoulos, L. Torner, and M. Soljacic, *Opt. Lett.* **33**, 1762 (2008).
17. P. J. Olver, *Applications of Lie Groups to Differential Equations*, 2nd edition (Springer Verlag, 1993).
18. M. J. Ablowitz and H. Segur, *Solitons and the Inverse Scattering Transform* (SIAM, 1981).
19. R. C. Davidson, *Methods in Nonlinear Plasma Theory* (Academic Press, 1972).
20. A. I. Maimistov, *Opt. Spectrosc.* **94**, 251 (2003).
21. N. G. Vakhitov and A. A. Kolokolov, *Radiophys. Quantum Electron* **16**, 783 (1973).
22. J. Yang, *Nonlinear Waves in Integrable and Non-integrable Systems* (SIAM, 2010).
23. M. Grillakis, J. Shatah, and W. Strauss, *J. Funct. Anal.* **74**, 160 (1987).
24. P. G. Kevrekidis, D. J. Frantzeskakis, and R. Carretero-González, *The Defocusing Nonlinear Schrödinger Equation* (SIAM, 2015).
25. D. E. Pelinovsky, R. M. Ross, and P. G. Kevrekidis, *J. Phys. A: Math. Theor.* **54**, 445701 (2021).
26. J. Yang and D. J. Kaup, *SIAM J. Appl. Math.* **60**, 967 (2000).